ELSEVIER

Biochemical Pharmacology 65 (2003) 551–561

Biochemical Pharmacology

www.elsevier.com/locate/biochempharm

The voltage- and time-dependent blocking effect of trifluoperazine on T lymphocyte Kv1.3 channels

Andrzej Teisseyre*, Krystyna Michalak

Department of Biophysics, Wrocław Medical University, ul. Chałubińskiego 10, 50-368 Wrocław, Poland

Received 18 July 2002; accepted 23 October 2002

Abstract

Phenothiazines are well-known calmodulin inhibitors that interact with many receptors and channels including a variety of potassium channels. In this study, we report a blocking effect of trifluoperazine (TFP) on voltage-gated Kv1.3 channels expressed in human T lymphocytes. Application of TFP in the concentration range from 1 to 20 μM reduced the current amplitude to about a half of the control value. The currents were blocked to less than 0.05 of the control value at 50 μM TFP concentration. The blocking effect was accompanied by a substantial increase in the current inactivation rate, whereas the activation rate and the steady-state activation and inactivation were not changed significantly. The blocking effect of TFP was voltage dependent being most potent at +60 mV and least potent at −20 mV. The blocking effect of TFP on the currents and the recovery from block was time dependent. Other calmodulin antagonists: tamoxifen (TMX) and thioridazine also inhibited the channels at micromolar concentrations. The effects exerted by TMX and thioridazine resembled the inhibitory effect of TFP. The blocking effect of thioridazine was time dependent and appeared to be more potent that the inhibition by TFP and TMX. TFP, TMX and thioridazine inhibited the activity of Kv1.3 channels only when applied extracellularly. The inhibitory effect of all the compounds was reversible. The possible physiological significance of the current inhibition is discussed.

Keywords: Phenothiazines; Trifluoperazine; T lymphocyte; Potassium channel; Patch-clamp

1. Introduction

Phenothiazines are well-known calmodulin inhibitors that are widely applied as antipsychotic agents, in particular in therapy of schizophrenia. It is thought that the therapeutic effects of phenothiazines are related to the blockade of dopamine receptors that are present in the central nervous system, particularly the D_2 subpopulation [1,2]. It is also known that phenothiazines exert immunomodulatory effects [3–5].

Apart from blocking effect on dopamine receptors, phenothiazines affect many other receptors in the central nervous system, including serotonin, α-adrenergic and histamine receptors [6], $GABA_A$ receptors [7] and ionotropic glutamate receptors [8,9]. It was shown that chlorpromazine blocks voltage-gated sodium channels in freshly isolated striatal neurons of the adult guinea-pig [10]. Chlorpromazine also blocks voltage-gated sodium, potassium and calcium channels in the neuroblastoma cell line N1E-115 [11].

Phenothiazines are also a blocker of a variety of potassium channels. It was shown that ''maxi'' calcium-activated channels expressed in dog airway smooth muscle are blocked by TFP and chlorpromazine [12]. Moreover, TFP blocks ''maxi'' calcium-activated potassium channels in pregnant rat myometrium, in rat hippocampal pyramidal neurons and in the internodal cells in charotype plants [13–15], as well as intermediate-conductance calcium-activated potassium channels in human TL [16]. It was also shown that TFP, trifluoperidol and pimozide block voltage-gated Kv2.1 channels expressed in human neurons

* Corresponding author. Tel.: +48-71-784-14-14; fax: +48-71-784-00-88.

E-mail address: ateiss@biofiz.am.wroc.pl (A. Teisseyre).

Abbreviations: TL, human T lymphocyte; 4-AP, 4-aminopyridine; TFP, trifluoperazine; TMX, tamoxifen; I_{rel}, relative peak current; I, current amplitude; $I_{contr60}$, current amplitude recorded on the same cell under control conditions at +60 mV; gK_{norm}, normalised relative chord conductance; gK, chord conductance; gK_{60}, chord conductance recorded on the same cell at +60 mV; gK_{-120}, chord conductance recorded on the same cell from the holding potential of −120 mV; V, membrane potential; V_{rev}, reversal potential of the current; V_n, activation midpoint; k_n, steepness of the voltage dependence (activation); τ_n, activation time constant; V_i, inactivation midpoint; k_i, steepness of the voltage dependence (inactivation); τ_i, inactivation time constant.

0006-2952/02/$ – see front matter
PII: S0006-2952(02)01561-7

[17]. Interestingly, these blocking effects of phenothiazines are due to direct interactions with the channels and occur independently to calmodulin inhibition.

The influence of phenothiazines on potassium channels in T lymphocytes was not fully investigated. Among several types of potassium channels expressed in human TL the most widely studied are voltage-gated channels termed Kv1.3 [18–20]. Available data provide evidence that the activity of Kv1.3 channels is necessary for setting the resting membrane potential in TL and is also required for the cell mitogenesis and volume regulation [18–20]. It is known that blockade of Kv1.3 channels also inhibits both the cell mitogenesis and volume regulation [18–20]. Therefore, some non-peptide Kv1.3 channel blockers have been tested as immunosuppresive agents [18–20]. Results obtained for TL cell line Jurkat indicate that a reduction of Kv1.3 channel activity mediated by the Src-like tyrosine kinase p56lck phosphorylation is involved in Fas-induced cell apoptosis [21,22].

First, indirect evidence for blocking effects of phenothiazines on TL potassium channels came from studies on mechanisms of the cell volume regulation [23]. It was shown that TFP, chlorpromazine and pimozide block the regulatory volume decrease in TL and that was due to a block of the potassium efflux during regulatory volume decrease [23]. However, it remained unclear whether these effects were related to calmodulin inhibition. Results of "patch-clamp" studies indicated that calmodulin antagonists: chlorpromazine and TFP blocked the channels as well as calcium channels blockers (e.g. verapamil) and that was due to a direct blocking effect on the channels [24]. However, the mechanism of the blocking effect of calmodulin antagonists was not studied in detail.

The aim of our study was to investigate the mechanism of TFP influence on Kv1.3 channels in human TL. The results provide evidence that application of TFP at micromolar concentration blocks the channels. The blocking process occurs in a voltage- and time-dependent manner.

2. Materials and methods

2.1. Cell separation, solutions and pipettes

Human TL were separated from peripheral blood samples from eight healthy donors using a standard method described elsewhere [25]. After separation, cells were cultured for at least 24 hr in the standard RPMI-1640 Medium (SIGMA) supplemented with 5% (v/v) Horse Serum (SIGMA).

Upon experiment, cells were placed in the external solution containing (in mM: 150 NaCl, 4.5 KCl, 1 $CaCl_2$, 1 $MgCl_2$, 10 HEPES, pH 7.35, 300 mOsm). The pipette solution contained (in mM: 70 KF, 80 KCl, 1 $CaCl_2$, 1 $MgCl_2$, 10 HEPES, 10 EGTA, pH 7.2, 280 mOsm). The free calcium concentration in the internal solution was calculated to be 100 nM. The chemicals were provided by the Polish Chemical Co (POCH), except of HEPES and EGTA that were purchased from SIGMA. TFP was purchased from ICN Biomedicals. Tamoxifen and thioridazine were purchased from SIGMA. Dishes with cells were placed under an inverted Olympus IMT-2 microscope. TFP containing solutions were applied using a fast perfusion system RSC 200 (Bio-Logic). Pipettes were pulled from the borosilicate glass and fire-polished before the experiment. The pipette resistance was in the range of 3–5 MΩ.

2.2. Electrophysiological recordings

Whole-cell potassium currents in TL were recorded applying the patch-clamp technique [26]. The currents were recorded using an EPC-7 Amplifier (List Electronics), low-pass filtered at 3 kHz, digitised using the LAB MASTER TL-1 (Axon Instruments) analog-to-digital converter with the sampling rate of 10 kHz and stored on the computer hard disk. A standard protocol of depolarising voltage stimuli contained seven pulses in the voltage range from −60 to +60 mV (20 mV increment) applied every 10 s, pulse duration 50 ms, holding potential −90 mV. The linear (ohmic) component of the current was subtracted on-line from the final record. The pulse duration was shortened to 40 ms in experiments performed with TMX and thioridazine. It is known that in the case of Kv1.3 channels, a "cumulative" or use-dependent inactivation may appear additionally to the "normal" inactivation [18–20]. The kinetics of "cumulative" inactivation are relatively slow compared to the "normal" inactivation and the recovery is extremely slow (time constant of ca. 420 s) [18–20]. The appearance of "cumulative" inactivation in our experiments would reduce the current amplitude in addition to the TFP action. The "cumulative inactivation" can be abolished by applying short (80–200 ms) depolarising pulses and long (20–30 s) interpulse intervals [18–20]. In our experiments we used 50 or 40 ms pulses. Moreover, in order to prove whether the 10 s interpulse interval is long enough to avoid the "cumulative inactivation", the currents recorded under control conditions by application of the same depolarising pulses with 10 and 30 s interpulse intervals were compared. Obtained results demonstrate that the currents recorded when applying a 10 s interpulse interval did not differ significantly from those obtained with a 30 s interval. Thus, a 10 s interpulse interval is long enough to avoid the "cumulative" inactivation [27]. Inactivation kinetics under control conditions were studied by using another protocol containing seven long-lasting (1 s) depolarising pulses applied every 30 s in the range from 0 to +60 mV (10 mV increment, holding potential −90 mV). The linear (ohmic) component of the current was subtracted on-line by applying the P/4 procedure. Since the inactivation time constant is decreased to 10–15 ms upon TFP application, the standard 50 ms pulses were long enough to be used for studying the inactivation kinetics upon the

drug application. Steady-state inactivation was investigated by recording the currents at fully depolarising potential (+40 mV) after having applied various holding potentials in the range from −120 to 0 mV (10 mV increment) for 40 s. Reversal potential was estimated by applying a tail current protocol: every 10 s the membrane was briefly (30 ms) depolarised to +40 mV from the holding potential of −90 mV to fully activate the currents and then repolarised to various potentials in the range from −50 to −90 mV (pulse duration −120 ms, 10 mV increment).

The data are given as mean ± SE. All experiments were carried out at room temperature (22–24°).

2.3. Data analysis

Since the number of active channels was varying significantly among the cells, the current amplitudes were presented in terms of a relative current (I_{rel}) defined as: $I_{rel} = I/I_{contr60}$, where I, current amplitude; $I_{contr60}$, current amplitude recorded on the same cell under control conditions at membrane potential +60 mV. Steady-state activation of the channels was presented in terms of a normalised relative chord conductance (gK_{norm}) defined by an equation: $gK_{norm} = gK/gK_{60}$, where gK, chord conductance; gK_{60}, chord conductance recorded on the same cell under the same circumstances at the membrane potential of +60 mV. Steady-state inactivation of the channels was presented in terms of a normalised relative chord conductance (gK_{norm}) defined by an equation: $gK_{norm} = gK/gK_{-120}$, where gK, chord conductance recorded at the potential of +40 mV from a given holding potential; gK_{-120}, chord conductance recorded on the same cell under the same circumstances from the holding potential of −120 mV. The chord conductance was calculated according to the definition: $gK = I/(V-V_{rev})$, where I, amplitude of the current; V, membrane potential; V_{rev}, reversal potential of the current. The voltage dependence of steady-state activation was fitted by a Boltzmann function given by an equation: $gK_{norm}(V) = 1/(1 + \exp(-((V - V_n)/k_n)))$, where V_n, activation midoint; k_n, steepness of the voltage dependence. The activation kinetics were fitted by applying the power function given by an equation: $I(t) = I(1 - \exp(-t/\tau_n))^2$, where τ_n, activation time constant. The voltage dependence of steady-state inactivation was fitted by a Boltzmann function as in the case of steady-state activation with the inactivation midpoint (V_i) applied instead of V_n and steepness (k_i) applied instead of k_n. Inactivation kinetics were fitted by applying the single exponential function. Statistical analysis was performed applying the Student's unpaired t-test. The results were concerned statistically significant when $P < 0.05$.

3. Results

Fig. 1A shows an example of the whole-cell potassium currents recorded in a TL under control conditions applying a standard protocol of depolarising voltage stimuli described in Section 2. The currents are evoked upon membrane depolarisation from the holding potential of −90 mV to voltages higher than −40 mV and fully activated at all potentials more positive than −20 mV. The currents reversed at the potential near −80 mV. Effect of application of 10 μM TFP on the currents is depicted on Fig. 1B. The record was taken after 6 min of TFP application. The current amplitude is apparently reduced and this is accompanied by a pronounced acceleration of the inactivation rate of the currents whereas the activation rate remains unchanged. It is presented more clearly in Fig. 1C, where the normalised currents recorded under control conditions and in the presence of 10 μM TFP at +60 mV are depicted.

In order to demonstrate that the recorded currents are predominantly carried by potassium ions, tail currents in the absence and presence of TFP were recorded applying a tail current protocol (Section 2). Fig. 2A and B depict an example of tail currents recorded under control conditions and upon application of 10 μM TFP, respectively. Fig. 2C shows the tail current amplitudes in the absence and presence of 10 μM TFP as a function of membrane potential. It can be seen that the current amplitude is reduced upon TFP treatment, but the reversal potential is not changed significantly. The estimated value of the reversal potential under control conditions and in the presence of 10 μM TFP is −78.1 ± 1.33 mV (N = 5) and −78.9 ± 1.43 mV (N = 5), respectively. This value is close to the estimated equilibrium potential for potassium ions under physiological conditions (−87 mV). Experiments performed previously in our laboratory under control conditions provided evidence that the currents are blocked to >95% upon application of 5 mM 4-AP, which selectively blocks Kv1.3 channels in human TL [27]. This is in agreement with results of other studies [18]. It is known that calcium-activated potassium channels termed IKCa1 are expressed abundantly in mitogen-activated TL [18–20]. IKCa1 channels are selectively blocked by clotrimazole at nanomolar concentrations [16]. Our results demonstrate that application of 500 nM clotrimazole does not reduce the currents significantly [27]. Moreover, the concentration of free calcium in the pipette solution was kept at the level of 100 nM (Section 2). This is below the activation threshold for IKCa1 channels [18,20]. All these results confirm that the currents recorded in our experiments are predominantly due to activation of Kv1.3 channels and argue against any significant contribution of IKCa1 currents.

The blocking effect of TFP is both concentration and time dependent. Fig. 3A depicts the relative peak currents at +60 mV as a function of a logarithm of TFP concentration. Upon application of 1, 2, 10 and 20 μM TFP, the relative current was decreased to 0.60 ± 0.024 (N = 5), 0.57 ± 0.021 (N = 5), 0.49 ± 0.033 (N = 10) and 0.54 ± 0.023 (N = 10) of the control value, respectively. When

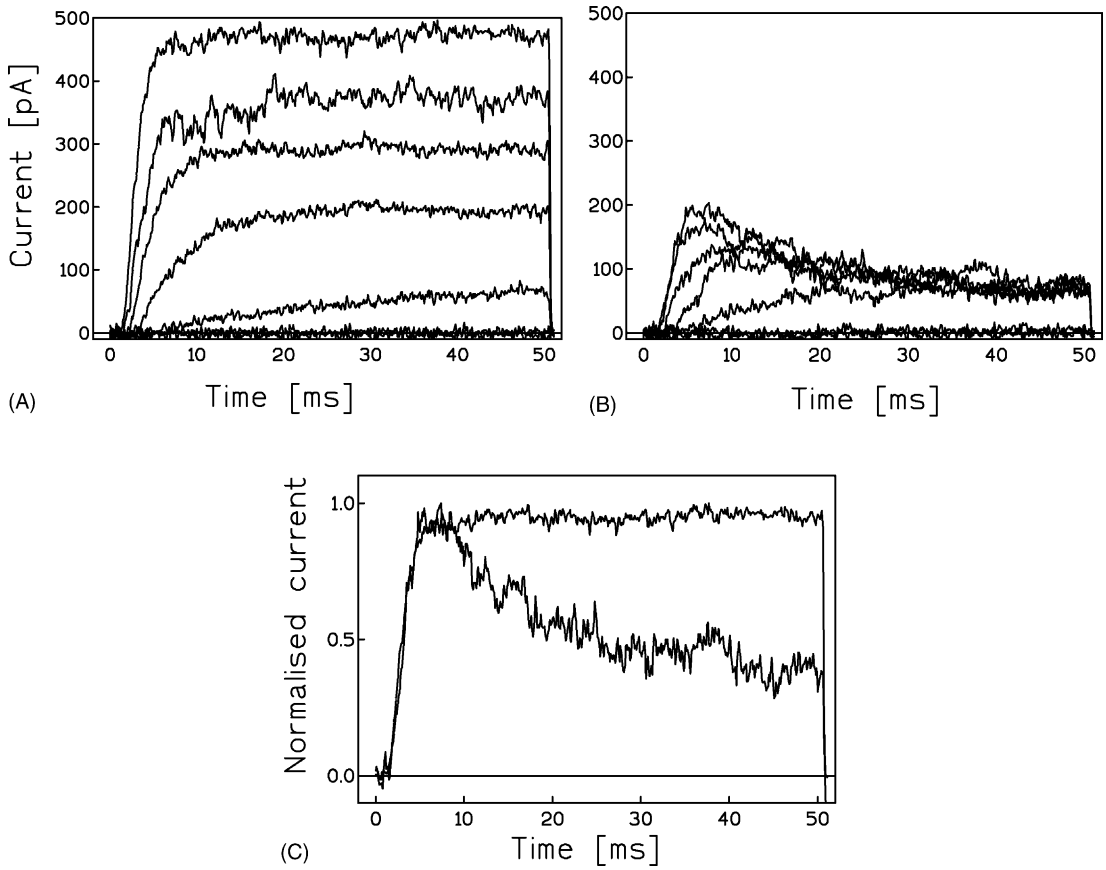

Fig. 1. TFP reduces whole-cell potassium currents in TL (A) control record obtained applying a standard protocol, (B) after 6 min of a continuous application of 10 μM TFP, (C) normalised currents recorded at +60 mV in the absence and presence of TFP.

raising TFP concentration to 40, 50 and 100 μM, the relative current was decreased to 0.1175 ± 0.03 (N = 5), 0.036 ± 0.015 (N = 5) and 0.0227 ± 0.016 of the control value, respectively (see also Fig. 3A). The decrease of the current amplitude was statistically significant ($P < 0.05$) at all the concentrations. Fig. 3B depicts the relative peak current at +60 mV as a function of time at 20 μM TFP concentration. The current was decreased to 0.66 ± 0.044 (N = 10) of the control value after 30 s of TFP application. This decrease was statistically significant ($P < 0.05$). When raising the time of TFP application to 120 and 240 s, the current amplitude was decreased to 0.54 ± 0.023 and 0.48 ± 0.073 of the control value, respectively (N = 10). This amplitude decrease was statistically significant from that recorded after 30 s of TFP application ($P < 0.05$).

The blocking effect of TFP is voltage dependent. Fig. 3C depicts the relative current amplitudes recorded in the presence of 20 μM TFP after 2 min of the drug application divided by the values recorded at the same potential under control conditions plotted as a function of the membrane potential. The current amplitude at −20 mV is almost unchanged (0.99 ± 0.01 of the control value) upon TFP application (N = 10, $P > 0.4$). The relative current amplitude is decreased to 0.89 ± 0.022 at 0 mV. This decrease is near the borderline of statistical significance (N = 10, $P = 0.033$). Upon the membrane depolarisation to +20, +40 and +60 mV, the current amplitudes are reduced to 0.69 ± 0.03, 0.59 ± 0.022 and 0.54 ± 0.023 of the control value, respectively (N = 10). The reduction is statistically significant ($P < 0.05$) for all the voltages. Raising TFP concentration to 40, 50 and 100 μM or increasing the time of application to 4 min produces a significant decrease of the current also at −20 and 0 mV (not shown). In general, the blocking effect of TFP is always most potent at +60 mV and least potent at −20 mV.

As it was mentioned previously, the inhibitory effect of TFP on the currents is accompanied by a significant increase in the current inactivation rate. It is known that the inactivation process of Kv1.3 channels is relatively slow (time constant of ca. 200 ms) and is weakly voltage dependent [18–20]. Fig. 4A depicts the inactivation time constant as a function of membrane potential under control conditions and in the presence of 20 μM TFP after 2 min of the drug application. It can be seen that the inactivation time constants were reduced from ca. 200 ms under control conditions to 10–20 ms upon TFP application. The reduction of the inactivation time constant is statistically significant for all membrane potentials in the range from 0 to +60 mV ($P < 0.05$). Fig. 4B depicts the activation time constants estimated for control records and upon application of 20 μM TFP after 2 min of the drug application. In

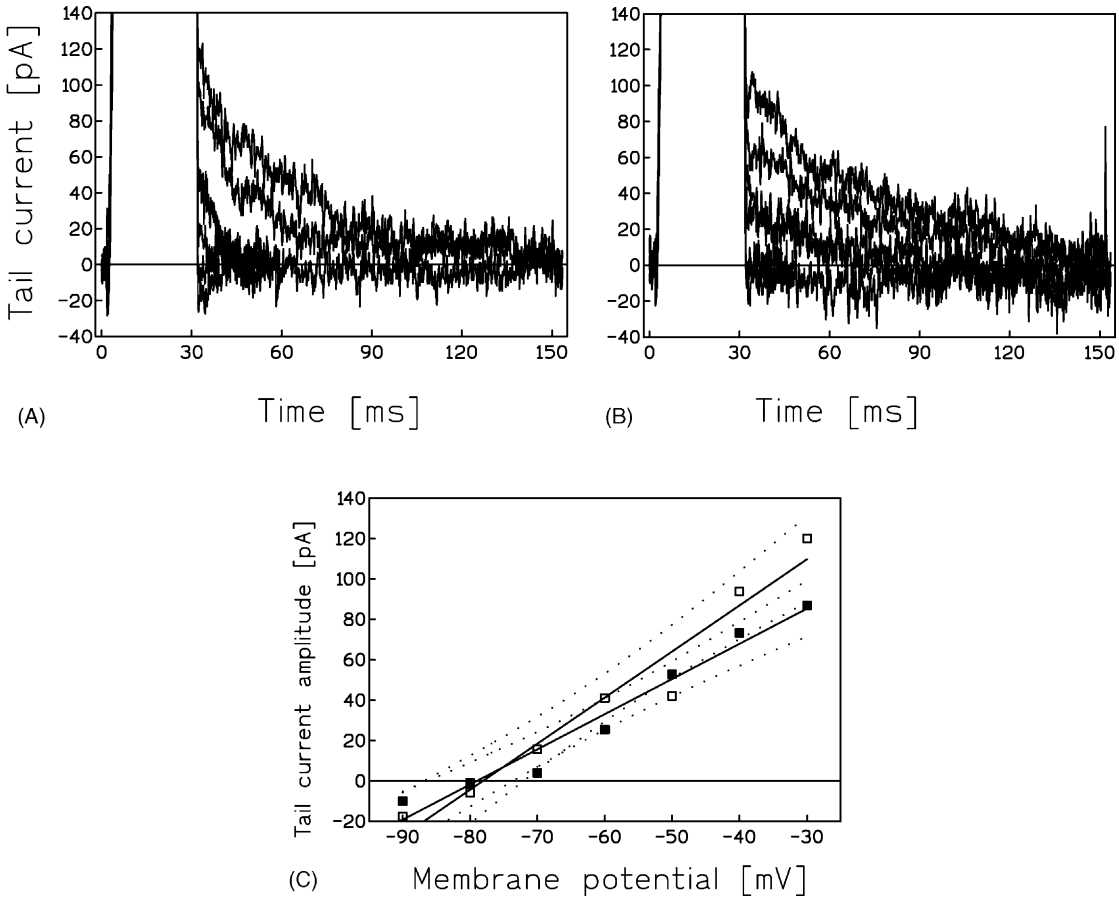

Fig. 2. Tail currents recorded in TL under control conditions (A) and in the presence of 10 μM TFP (B). (C) Tail current amplitude estimated from control records (□) and upon application of 10 μM TFP (■) as a function of membrane potential.

contrast to the inactivation process, the activation kinetics were not changed significantly upon TFP treatment ($P > 0.05$).

Influence of TFP application on the steady-state activation and inactivation was also investigated. Fig. 5A shows the steady-state activation in terms of the relative chord conductance normalised to 1 at +60 mV as a function of membrane potential. Under control conditions, the activation midpoint (V_n) parameter is -15.24 ± 0.84 mV and the steepness (k_n) parameter is 6.83 ± 0.74 mV (N = 10). Application of 10 μM TFP changes the V_n parameter to ca. −20 mV and the k_n to ca. 2 mV (an accurate estimation was not possible because of a big standard error). The changes in the V_n and k_n parameters do not depend on time of TFP application. These changes are not significant ($P > 0.05$) and are rather due to the fact that the blocking effect of TFP is less potent at −20 and 0 mV than at positive potentials, so the value of normalised chord conductance at −20 and 0 mV is much bigger upon TFP application than under control conditions. This increases also the steepness of the curve (see Fig. 5A). Fig. 5B depicts the steady-state inactivation in terms of the relative chord conductance normalised to 1 at holding potential of −120 mV as a function of holding potential. The inactivation midpoint (V_i) parameter under control conditions and upon application of 10 μM TFP is -68.37 ± 0.52 and -64.26 ± 1.33 mV, respectively (N = 5). The steepness parameter (k_i) is -7.03 ± 0.44 and -5.77 ± 1.28 mV, respectively (N = 5). Also in the case of steady-state inactivation the influence of TFP treatment was not significant ($P > 0.05$).

Recovery from block is time dependent. Fig. 6 shows the recovery process after wash-out of 2 μM TFP. Application of TFP for 2 min reduces the relative currents at +60 mV to 0.40 ± 0.067 (N = 5) of the control value. The wash-out of TFP for 30 s restores the currents to only about 70% of control values. Raising the time of wash-out to 4 min increases the degree of recovery to more than 90%. When increasing the TFP concentration to 20 μM, the current amplitudes recovered to 90–95% of the control values after 2–4 min of wash-out of the drug (not shown). The current amplitude recorded after 4 min of wash-out was not significantly different from the control value ($P > 0.05$). This indicates that the blocking effect of TFP is reversible.

In order to elucidate whether TFP inhibits the channels acting from the extracellular or intracellular side of the membrane, 20 μM TFP was added to the intracellular (pipette) solution. It is known that when performing the whole-cell recording the cell interior is dialysed with the pipette solution and this dialysis is complete within

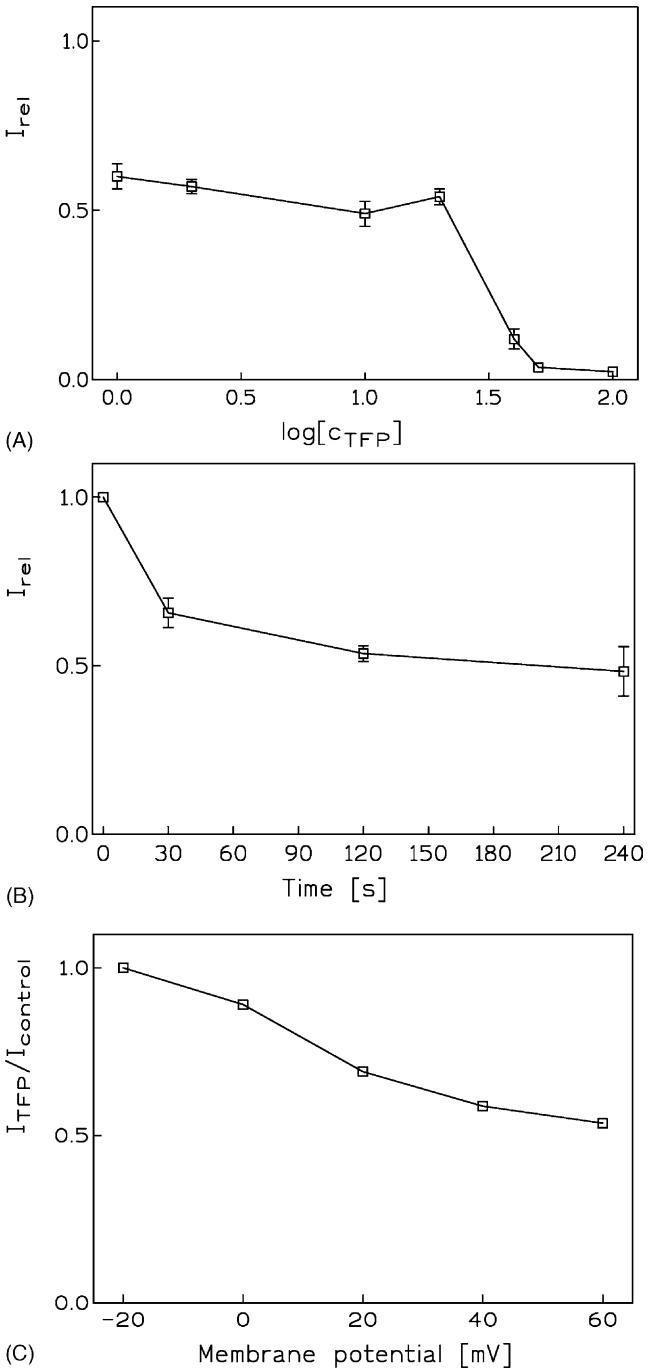

Fig. 3. (A) Concentration dependence of the blocking effect of TFP. The relative peak current defined in Section 2 recorded at +60 mV after 2 min of TFP application plotted vs. the logarithm of TFP concentration. (B) Time dependence of the relative current at +60 mV at 20 μM TFP concentration. (C) The voltage dependence of the relative peak current defined in Section 3 recorded in the presence of 20 μM TFP after 2 min of the drug application. The data in A–C was fitted by a point-to-point line.

1.5–4 min after break-in to whole-cell [28]. Thus, if TFP affected the channels from the intracellular side, an inhibitory effect should be observed after a couple of minutes of the whole-cell recording. In contrast, as can be seen in Fig. 7A, the intracellular application of TFP does not affect the currents significantly for at least 20 min of the whole-cell recording ($P > 0.05$). In another experiment, 20 μM TFP was added to the pipette and, after having performed the first recording protocol, 20 μM TFP was also applied extracellularly. As can be seen in Fig. 7B, the extracellular application of TFP inhibits the currents to ca. 50% of the control value after 2 min of drug application. After wash-out of TFP from the extracellular space, the currents almost fully recovered to their control values. These results are indistinguishable from those obtained in the absence of TFP in the intracellular solution. These observations argue against any action of TFP from the intracellular side and indicate that TFP inhibits the channels by acting from the extracellular side.

The effects of other calmodulin antagonists—TMX and thioridazine [29,30] on the Kv1.3 channels were also studied. Fig. 8A–B depict the control records and the effect of an application of 20 μM TMX on the currents, respectively. The record in the presence of TMX was performed 30 s after the drug application. The current amplitude is apparently reduced upon TMX application and, similarly to what happens in case of TFP application, this reduction is accompanied by a pronounced increase in the current inactivation rate, whereas the activation rate remains unchanged (see Fig. 8C). Fig. 8D shows the relative peak currents obtained upon an application of 20 μM TMX divided by the value recorded under control conditions, as a function of membrane potential. As can be seen, the inhibitory effect of TMX is voltage dependent. TMX application decreases the current to 0.91 ± 0.023 of the control value at −20 mV ($P = 0.03$, near the borderline of statistical significance). Upon membrane depolarisation to 0, +20, +40 and +60 mV, the relative peak current is decreased to 0.74 ± 0.02, 0.65 ± 0.033, 0.61 ± 0.02 and 0.6 ± 0.01 ($N = 5$) of the control value, respectively. The current decrease for all the voltages is statistically significant ($P < 0.05$). Fig. 9A–B show the effect of TMX application on the current activation and inactivation time constants, respectively. It can be seen that the activation time constant remains unchanged upon TMX treatment ($P > 0.05$), whereas the inactivation rate is significantly ($P < 0.05$) reduced at +40 and +60 mV. The decrease of the inactivation rate at +20 mV is not significant ($P > 0.05$) due to a big scatter of the data and the value obtained at 0 mV is not significantly different from the control ($P > 0.05$). The inhibitory effect of TMX is reversible (not shown).

Fig. 10A–B depict the records obtained under control conditions and upon an application of 20 μM thioridazine, respectively. The record in the presence of thioridazine was performed 30 s after the drug application. The current amplitude is significantly reduced upon thioridazine application and the inhibitory effect seems to be more pronounced than upon application of the same concentration of TMX (see also Fig. 10D). Similarly to TFP and TMX treatment, the current reduction is accompanied by a pronounced increase in the inactivation rate, whereas the

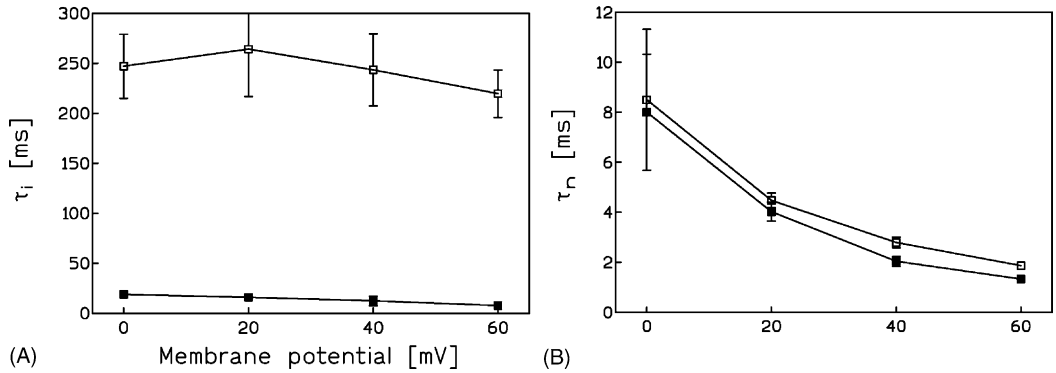

Fig. 4. (A) Inactivation time constants as a function of membrane potential under control conditions (□) and upon application of 20 μM (N = 10) TFP (■). (B) Activation time constants as a function of membrane potential estimated for control records (□) and upon application of 20 μM (N = 10) TFP (■). The data depicted in A–B upon TFP application was estimated for records obtained after 2 min of the drug application. The data presented in A–B was fitted by a point-to-point line.

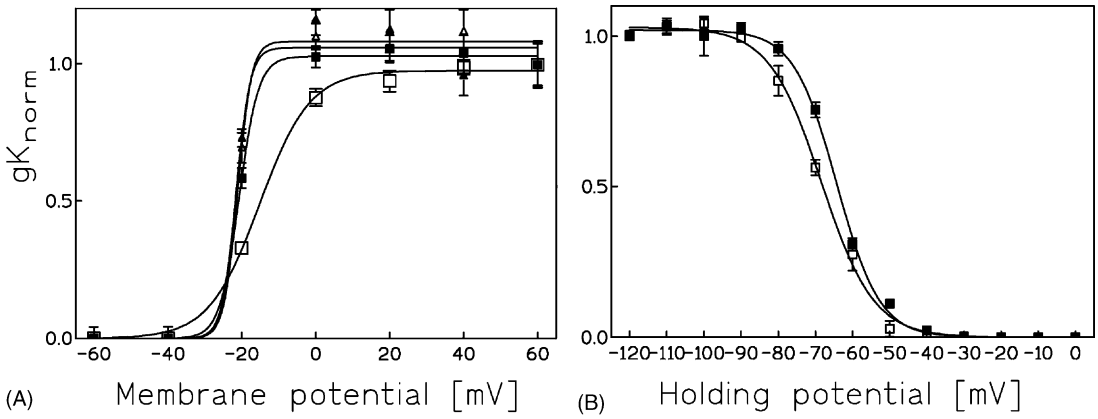

Fig. 5. (A) Steady-state activation in terms of normalised relative chord conductance vs. the membrane potential. (□) control conditions; (■) (△) and (▲) −30 s, 2 and 4 min after continuous application of 10 μM TFP, respectively (N = 10). (B) Steady-state inactivation in terms of normalised relative chord conductance vs. the holding potential. (□) Control conditions; (■) application of 10 μM TFP (N = 5).

activation rate remains unchanged (see Fig. 10C). Fig. 10D shows the relative peak currents upon application of 20 μM thioridazine divided by the currents recorded under control conditions, as a function of membrane potential. The

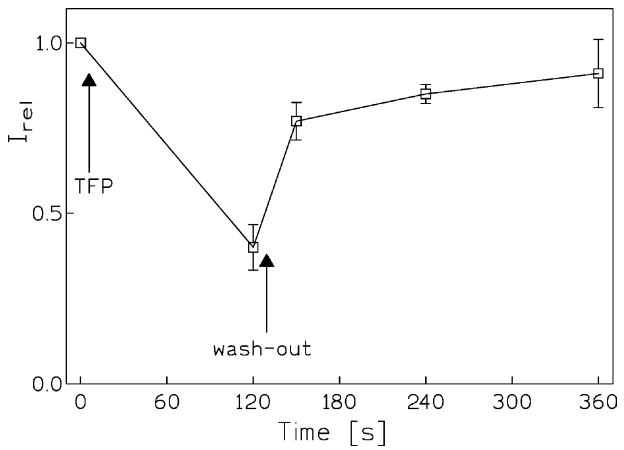

Fig. 6. Recovery from block by TFP as a function of time. Application of 2 μM TFP (N = 5) and wash-out is indicated by an arrow. The data was fitted by a point-to-point line.

inhibitory effect of thioridazine is voltage dependent, the drug is least effective at −20 mV and most effective at +60 mV. The reduction of the current amplitude is statistically significant ($P < 0.05$) for all the potentials. The fraction of unblocked current in the presence of 20 μM thioridazine recorded at +60 mV after 30 s of the drug application is 0.38 ± 0.1 (N = 5). This is significantly ($P < 0.05$) less than the reduction upon TFP and TMX application. Altogether, obtained data may suggest that thioridazine is more potent blocker of Kv1.3 channels than TFP and TMX. Moreover, the blocking effect of thioridazine is also time dependent. The current amplitudes are significantly ($P < 0.05$) lower after 2 min of a continuous thioridazine application than recorded after 30 s of the drug application (see Fig. 10D). The fraction of unblocked current in the presence of 20 μM thioridazine recorded at +60 mV after 2 min of the drug application is 0.26 ± 0.034 (N = 5). Fig. 11A–B show the effect of thioridazine application on the current activation and inactivation time constants, respectively. It can be seen that the activation time constant remains unaffected ($P > 0.05$) upon drug application, whereas the inactivation time constant is

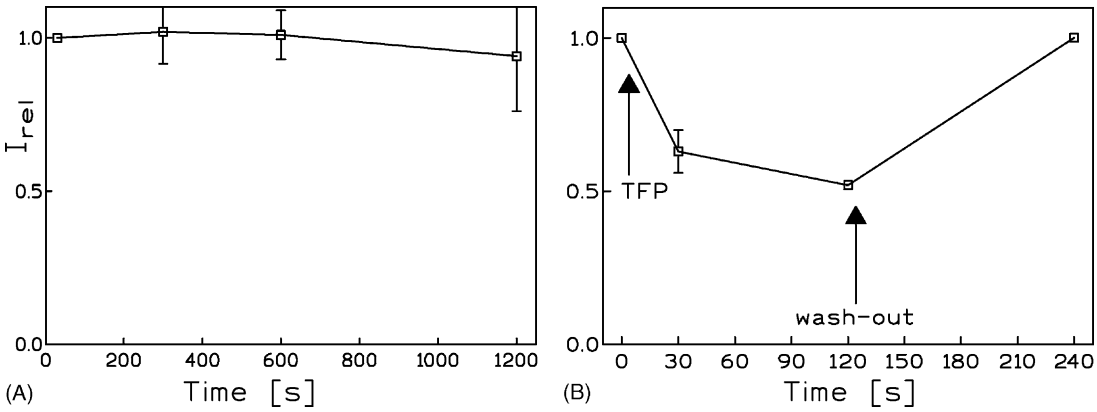

Fig. 7. (A) Relative peak currents recorded at +60 mV in the presence of 20 μM TFP in the pipette solution as a function of time (N = 2). (B) The currents recorded in the presence of 20 μM TFP in the pipette solution. An extracellular application of 20 μM TFP and wash-out is indicated by an arrow (N = 5). The data presented in A–B was fitted by a point-to-point line.

reduced at positive potentials to ca. 15–7 ms after 30 s of the drug application. The reduction of the inactivation rate is statistically significant ($P < 0.05$) for all the potentials. The inhibitory effect of thioridazine application is reversible (not shown).

Both TMX and thioridazine were effective only when applied from the extracellular side. Application of either of the drug to the intracellular solution neither inhibited the currents, nor it influenced the effect of the drug application from the extracellular side (not shown).

4. Discussion

Results of our study demonstrate that TFP blocks TL potassium channels in a concentration, voltage- and time-dependent manner. The blocking effect on whole-cell potassium currents is accompanied by a substantial acceleration of inactivation kinetics, whereas activation kinetics remains unaffected upon TFP treatment. Also the voltage dependence of steady-state activation and inactivation are not altered in the presence of TFP. The blocking effect of

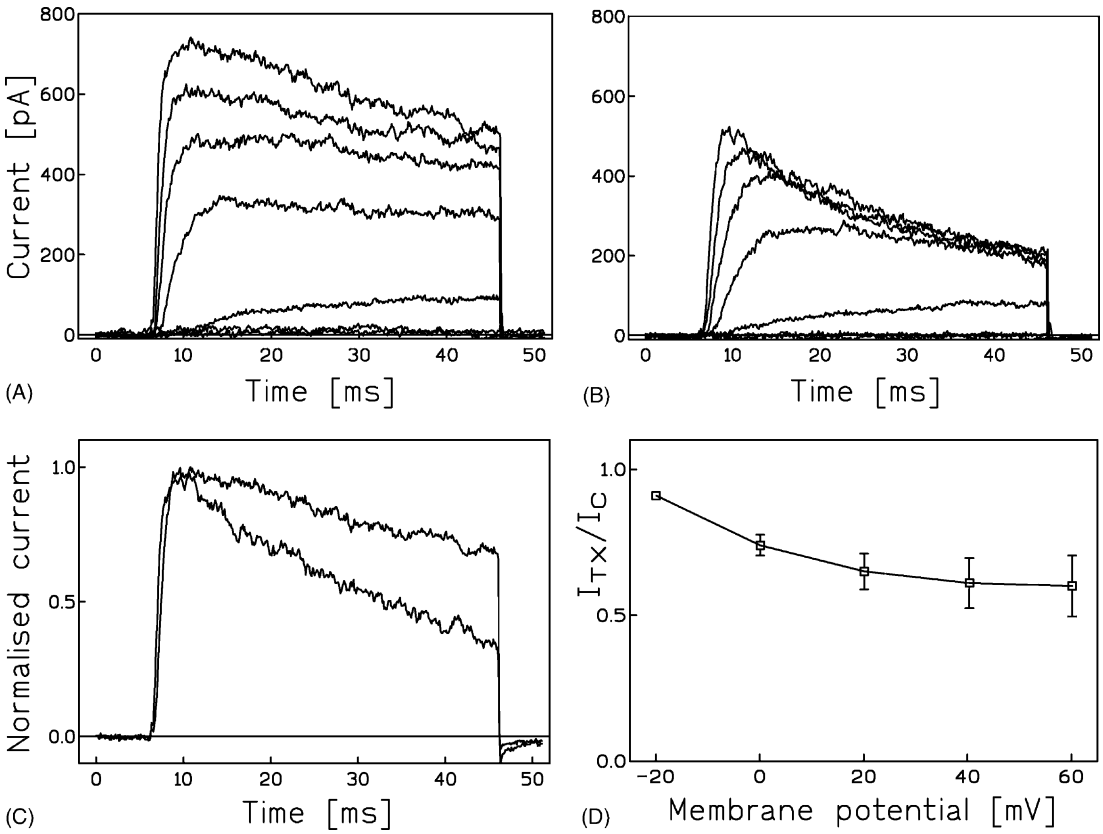

Fig. 8. Inhibition of the whole-cell potassium currents in TL by TMX (A) control record, (B) after 30 s of an application of 20 μM TMX, (C) normalised currents recorded at +60 mV in the absence and presence of TMX, (D) relative peak currents defined in Section 3 (I_{TX}/I_C) as a function of membrane potential (N = 5). The data in D was fitted by a point-to-point line.

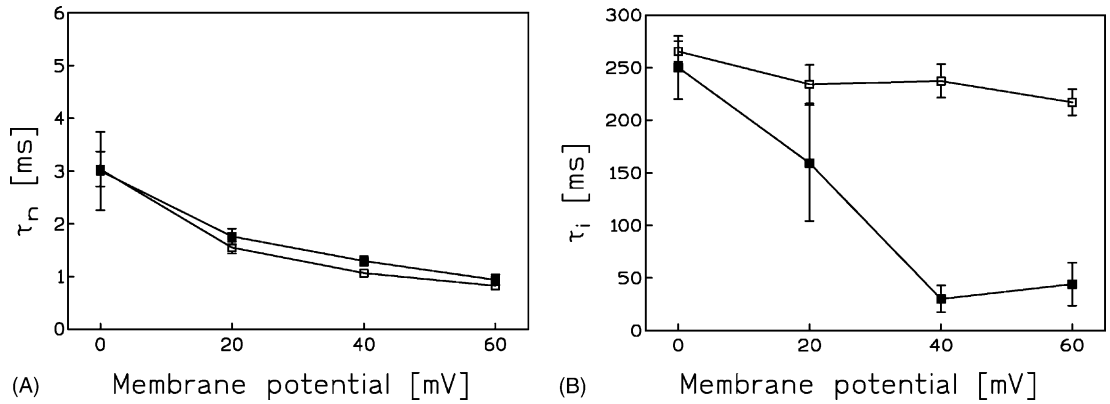

Fig. 9. (A) Activation time constants as a function of membrane potential, □ control conditions (N = 5), (■) 30 s after application of 20 μM TMX (N = 5). (B) Inactivation time constants as a function of membrane potential: (□) control conditions; (■) 30 s after application of 20 μM TMX (N = 5). The data in A and B was fitted by a point-to-point line.

TFP occurs at micromolar concentrations and is reversible. Other calmodulin antagonists: TMX and thioridazine also inhibit the currents. The inhibition of the currents by TMX and thioridazine resembles the effect of TFP. In both cases, the inhibitory effect on the currents is accompanied by a pronounced acceleration of the inactivation rate, whereas the activation rate is not changed significantly. The blocking effect of thioridazine is time dependent and seems to be more potent than the inhibition by TFP and TMX. Moreover, all the drugs are effective only when applied from the extracellular side.

It is known that TFP is cytotoxic and the cytotoxicity can be estimated using several criteria [3]. The level of TFP cytotoxicity depends on concentration. TFP was shown to be always cytotoxic according to all criteria at 100 μM, occasionally cytotoxic at 25 μM and rarely toxic at 1 and 10 μM [3]. Therefore, the concentration range from 1 to 10 μM was chosen as non-toxic for experiments in which cells were incubated in the presence of TFP up to 24 hr [3]. The blocking effect of TFP reported in our study occurred both at non-toxic and toxic concentrations. Moreover, the time of cell superfusion with TFP-containing solutions was

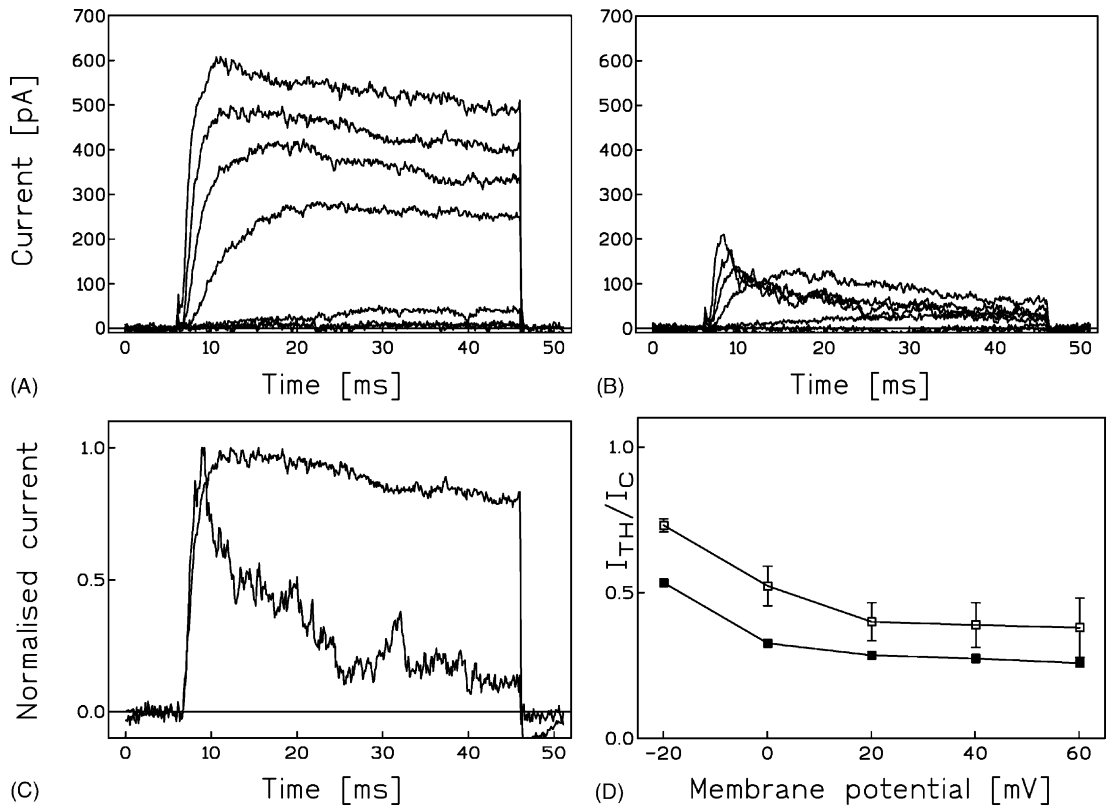

Fig. 10. The inhibitory effect of thioridazine on the currents in TL (A) control record, (B) after 30 s of an application of 20 μM thioridazine, (C) normalised currents recorded at +40 mV in the absence and presence of thioridazine, (D) relative peak current defined in Section 3 (I_{TH}/I_C) as a function of membrane potential: (□) 30 s, (■) 2 min after application of 20 μM thioridazine, respectively (N = 5). The data in D was fitted by a point-to-point line.

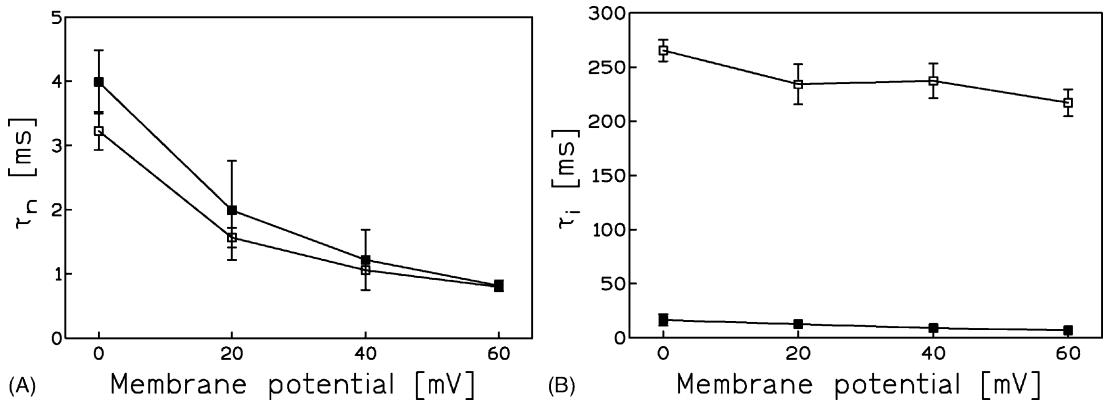

Fig. 11. (A) Activation time constants as a function of membrane potential, (□) control conditions (N = 5), (■) 30 s after application of 20 μM thioridazine (N = 5). (B) Inactivation time constants as a function of membrane potential: (□) control conditions, (■) 30 s after application of 20 μM thioridazine (N = 5). The data in A and B was fitted by a point-to-point line.

never longer than 6 min. It can, therefore, be ruled out that the blocking effect of TFP in the concentration range from 1 to 20 μM is due to the cytotoxicity. Nevertheless, the cytotoxicity may contribute to the inhibitory effect exerted by TFP at concentrations higher than 20 μM.

Another possible way of TFP influence on the channels is the inhibitory effect on calmodulin. Application of 10 μM TFP inhibits the calmodulin-activated phosphodiesterase by 50% [31]. TMX and thioridazine are also calmodulin inhibitors [29,30]. Calmodulin is known to mediate activation of many types of ion channels. Experiments performed recently on potassium channels in TL demonstrate that calmodulin binds to C-tail and mediates activation of calcium-activated potassium channels, but does not bind to Kv1.3 channels [32]. Moreover, our data demonstrate that TFP, TMX and thioridazine act on the channels from the extracellular, but not from the intracellular side. Altogether, it may be suggested that calmodulin does not mediate the activation of Kv1.3 channels, so, the inhibition of calmodulin by TFP, TMX and thioridazine cannot mediate the channel inhibition. It is rather suggested that the blocking effect of the drugs is due to a direct effect on Kv1.3 channels.

It is known that TFP may block potassium channels via an ''open channel block'' mechanism. Such a block occurs in case of calcium-activated potassium channels expressed in dog airway smooth muscle cells [12] and in rat hippocampal pyramidal neurons [14]. According to that model, TFP blocks the open channels at micromolar concentrations from the intracellular, but not from the extracellular side [12,14]. The inhibitory effect of TFP on the channels is moderately voltage dependent [12,14].

Results of our study demonstrate, however, that the inhibitory effect of TFP, TMX and thioridazine on TL Kv1.3 channels differs significantly from the effect on rat hippocampal neurons. First, results our study demonstrate that the drugs inhibit the channels from the extracellular and not intracellular side. Also, in contrast to what is observed for rat hippocampal neurons, the inhibitory effect of TFP on Kv1.3 channels shows a weak concentration dependence in the range from 2 to 20 μM. In this concentration range the currents were blocked to about a half of their control values. Therefore, it was neither possible to accurately estimate the dissociation constant and the Hill's coefficient, nor it was possible to apply the Woodhull's equation to estimate the partition parameter δ. Moreover, the blocking effect of TFP observed in our study is clearly time dependent at any concentration used. Thus, the mechanism of the inhibitory effect of TFP, TMX and thioridazine on Kv1.3 channels can not be described properly using an ''open channel block'' formalism.

The blocking effect on Kv1.3 channels may be of physiological significance. It is known that potassium channels, both voltage- and calcium-activated contribute to TL mitogenesis and volume regulation [18–20]. Application of TFP and TMX at a concentration range of 1–10 μM inhibits TL mitogenesis [3,30]. Cell volume regulation is inhibited by 50% when applying TFP at a concentration of 3–5 μM [23]. Our results demonstrate that application of TFP in this concentration range is sufficient to reduce Kv1.3 currents substantially. Recently obtained results demonstrate that application of TFP in the similar range of concentration blocks calcium-activated potassium channels expressed abundantly in activated TL [16]. It can be concluded that application of TFP at micromolar concentrations blocks both voltage- and calcium-activated potassium channels in TL. These blocking effects are sufficient to inhibit both TL mitogenesis and volume regulation.

Other effect that is exerted by calmodulin antagonists: TFP and TMX is an inhibition of spontaneous apoptosis of CD4+ T cells in HIV-infected patients [33]. It is known that in HIV-infected individuals there is an increased spontaneous apoptosis of CD4+ T cells due to an increased activation-induced cell death [33]. Application of 7.5 μM TFP and TMX was shown to inhibit the spontaneous apoptosis of CD4+ T cells and to increase the ratio of CD4+/CD8+ cells in TL from HIV-infected patients [33].

The exact mechanism of this inhibition remains unknown. Nevertheless, recently performed experiments with CD4+ lymphoblastoid cell line CEM showed an increased expression of Kv1.3 channels and an increased Ca^{2+} content in ionomycin-sensitive intracellular stores in cells transfected with HIV-1 Nef protein [34]. The concentration of 7.5 μM TFP and TMX are sufficient to block both the Ca–calmodulin complex [29,30] and Kv1.3 channels (our study). This may inhibit the pathological activation of CD4+ cells that leads to an activation-induced cell death.

Acknowledgments

The authors would like to express best thanks to our colleague from the Biophysics Department-dr Andrzej Poła, who kindly provided the blood samples for lymphocyte isolation. This work was supported by the Polish State Committee for Scientific Research (KBN) funds for Wrocław Medical University for research activity and the University Grant No. 562.

References

[1] Seeman P. Brain dopamine receptors. Pharmacol Rev 1980;32:229.
[2] Billard W, Ruperto G, Crosby L, Iorio C, Barnett A. Characterisation of the binding of ^{3}H-SCH 23390, a selective D-1 receptor antagonist ligand, in rat striatum. Life Sci 1984;35:1885.
[3] Stavitsky A, Dasch J, Astrachan L. Effects of trifluoperazine a, calmodulin antagonist, on rabbit T- and B-cell responses to mitogens and antigen. Cell Immunol 1984;87:411–23.
[4] Molnar J, Mandi Y, Petri I, Petofi S, Sakagami H, Kurihara T, Motohashi N. Immunomodulation activity of phenothiazines, benzophenothiazines and benzacridines. Anticancer Res 1993;13:439–42.
[5] Petri I, Szekeres E, Berek I, Molnar J, Sakagami H, Motohashi N. Effect of benzophenothiazines on natural killer cell activity of human peripheral blood mononuclear cells. Anticancer Res 1993;13:2273–6.
[6] Peroutka S, Snyder SH. Relationship of neuroleptic drug effects at brain dopamine, serotonin, α-adrenergic and histamine receptors to clinical potency. Am J Psychiatry 1980;137:1518–22.
[7] Mozrzymas J, Barberis A, Michalak K, Cherubini E. Chlorpromazine inhibits miniature GABAergic currents by reducing the binding and increasing the unbinding rate of $GABA_A$ receptors. J Neurosci 1999; 19:2474–88.
[8] Żarnowska E, Mozrzymas J. Differential effects of chlorpromazine on ionotropic glutamate receptors in cultured rat hippocampal neurons. Neurosci Lett 2001;305:53–6.
[9] Żarnowska E, Mozrzymas J. Chlorpromazine prolongs the deactivation of *N*-methyl-D-aspartate-induced currents in cultured rat hippocampal neurons. Neurosci Lett 2001;315:1–4.
[10] Ogata N, Tatebayashi H. Modulation of sodium current kinetics by chlorpromazine in freshly-isolated striatal neurones of the adult guinea-pig. Br J Pharmacol 1989;98:1173–84.
[11] Ogata N, Yoshii M, Narahashi T. Psychotropic drugs block voltage-gated ion channels in neuroblastoma cells. Brain Res 1989;476:140–4.
[12] McCann J, Welsh M. Neuroleptics antagonize a calcium-activated potassium channel in airway smooth muscle. J Gen Physiol 1987;89: 339–52.
[13] Kihira M, Matsuzawa K, Tokuno H, Tomita T. Effects of calmodulin antagonists on calcium-activated potassium channels in pregnant rat myometrium. Br J Pharmacol 1990;100:353–9.
[14] Ikemoto Y, Yoshida A, Oda M. Blockade of trifluoperazine of a Ca-activated K^+ channels in rat hippocampal pyramidal neurons. Eur J Pharmacol 1992;216:191–8.
[15] Laver D, Cherry C, Walker N. The actions of calmodulin antagonists W-7 and TFP on the gating kinetics of the calcium-activated large-conductance potassium channel in the Chara protoplasmic drop: a substate-sensitive analysis. J Membr Biol 1997;155:263–74.
[16] Khanna R, Chang M, Joiner W, Kaczmarek L, Schlichter L. hSK4/hIK1, a calmodulin-binding K(Ca) channel in human T lymphocytes. J Biol Chem 1999;274(21):14838–49.
[17] Wible B, Murawsky M, Crumb W, Rampe D. Stable expression and characterization of the human brain potassium channel Kv2.1: blockade by antipsychotic agents. Brain Res 1997;761:42–50.
[18] Lewis R, Cahalan M. Potassium and calcium channels in lymphocytes. Annu Rev Immunol 1995;13:623–53.
[19] Teisseyre A. Voltage-gated potassium channels in T lymphocytes—physiological role and changes in channel properties in diseases. Cell Mol Biol Lett 1996;1:337–51.
[20] Teisseyre A. The "patch-clamp" technique and its application in investigations of the properties of human T lymphocyte potassium channels. Cell Mol Biol Lett 2001;6:93–105.
[21] Szabo I, Gulbins E, Apfel H, Zhang X, Barth P, Busch A, Schlottman K, Pongs O. Tyrosine phosphorylation-dependent suppression of a voltage-gated K^+ channel in T lymphocytes upon Fas stimulation. J Biol Chem 1996;271:20465–9.
[22] Gulbins E, Szabo I, Balzer K, Lang F. Ceramide-induced inhibition of T lymphocyte-gated potassium channel is mediated by tyrosine kinases. Proc Natl Acad Sci USA 1997;94:7661–6.
[23] Grinstein S, Dupre A, Rothstein A. Volume regulation by human lymphocytes—role of calcium. J Gen Physiol 1982;79:849–68.
[24] Cahalan MD, Lewis RS. Role of potassium and chloride channels in volume regulation by T lymphocytes, Chapter 24. Cell physiology of blood. The Rockefeller; 1988.
[25] Hirano T, Kuritani T, Kishimoto Y, Yamamura Y. T cell dependency of PWM-induced Ig production by B cells. J Immunol 1977;119:1235.
[26] Hamill O, Marty A, Neher E, Sakmann B, Sigworth F. Improved patch-clamp techniques for high-resolution current recording from cells and cell-free membrane patches. Pflügers Arch 1981;391:85–100.
[27] Teisseyre A, Mozrzymas JW. Inhibition of the activity of T lymphocyte Kv1.3 channels by extracellular zinc. Biochem Pharmacol 2002; 64:595–607.
[28] Verheugen J. Elevation of intracellular Ca in the physiologically relevant range does not inhibit voltage-gated K^+ channels in human T lymphocytes. J Physiol 1998;508:167–77.
[29] Baral E, Nagy E, Kwok S, McNicol A, Gerrard J, Berczi I. Suppression of lymphocyte mitogenesis by tamoxifen: studies on protein kinase C, calmodulin and calcium. Neuroimmunomodulation 2000; 7:68–76.
[30] Ashkenazy-Shakar M, Beitner R. Effects of Ca-ionophore A23187 and calmodulin antagonists on regulatory mechanisms of glycolysis and cell viability of NIH-3T3 fibroblasts. Mol Genet Metab 1999;67(4): 334–42.
[31] Weiss B, Levin R. Mechanisms for selectivity inhibiting the activation of cyclic nucleotide phosphodiesterase and adenylate cyclase by antipsychotic agents. Adv Cyclic Nucleotide Res 1978;9:285–303.
[32] Fanger Ch, Ghanshani S, Logsdon N, Rauer H, Kalman K, Zhou J, Beckingham K, Chandy K, Cahalan M, Aiyar J. Calmodulin mediates calcium-dependent activation of the intermediate-conductance K(Ca) channel IKCa1. J Biol Chem 1999;274(9):5746–54.
[33] Pan G, Zhou T, Radding W, Saag M, Mountz J, McDonald J. Calmodulin antagonists inhibit apoptosis of CD4+ T-cells from patients with AIDS. Immunopharmacology 1998;40:91–103.
[34] Zegarra-Moran O, Rasola A, Rogolo M, Porcelli A, Rossi B, Galietta L. HIV-1 Nef expression inhibits the activity of a Ca^{2+}-dependent K^+ channel involved in the control of the resting potential in CEM lymphocytes. J Immunol 1999;162:5359–66.